

Electromagnetic Radiation in Bio-Tissue: A Numerical implementation

Michele Buonsanti*, Giuseppe Megali and Matteo Cacciola

Department DICEAM University of Reggio Calabria, Italy Via Graziella loc. Feo di Vito 89060 Reggio Calabria, Italy

Abstract

Wireless personal communication is a rapidly expanding sector, particularly in the field of wireless local area networks. In an indoor wireless network system, an user can be close to the radiating antenna. Therefore, it is important to consider possible health hazards due to this type of exposure. This paper presents an approach to estimate and evaluate the main characteristics, i.e., Specific Absorption Rate and temperature rise, related to human exposure to electromagnetic field radiated by common wireless devices such as Wireless Access Points or Hot-Spot. The assessment is done numerically using two different approaches, respectively Ray-Tracing model and Finite Element Method. The general goal is to provide an efficient and accurate method to assess human head exposure to electromagnetic fields at a frequency of 2.45 GHz and for different types of exposure conditions.

Keywords: Electromagnetic radiation; Wi-Fi; FEM; Specific absorption rate; Bio-Tissue; Indoor

Introduction

In the recent years, wireless personal communications have registered a rapidly expansion particularly in the field of wireless local area networks (WLANs). The existing applications of WLANs are spread spectrum systems operating at the Industrial Scientific Medical (ISM) frequency (2.45GHz) and the Unlicensed National Information Infrastructure (U-NII) (5.5 GHz) [1].

Although this framework has given numerous advantages to people, the steadily increasing use of these new technologies may result in greater radio-frequency (RF) exposure in homes and work places. Health agencies have expressed their concern about cumulative exposure [2]. In this paper we focus our attention on the risks of human head exposure to such devices evaluating some important parameters, i.e., Specific Absorption Rate (SAR) and superficial temperature increasing. In this analysis, it is important to underline that WLAN systems use almost omni-directional antennas.

The user can be close to the radiating antenna, where the Electro Magnetic (EM) field assumes its highest values. As a consequence, it is important to consider the possible health hazard due to such systems and, in particular, to define criteria and thresholds for human safety [3]. Our goal is to verify if actual standards in wireless devices respect the Institute of Electrical and Electronic Engineers (IEEE), International Commission on Non-Ionizing Radiation Protection (ICNIRP) and European Committee for Electro technical Standardization (CENELEC) standards. Thus, our goal is to quantify the absorbed power by a biological organism exposed to a EM field and determine its distribution. For our purposes, we approached the problem in two steps. Firstly, we realized the indoor environment and set antenna specifications to evaluate EM field that propagates inside several scenarios. Afterward, retaining previously results, we exploited a FEM approach for simulating the EM absorption of a human head.

Magneto-Hydrodynamics and Physiological Basic Considerations

Red blood cells are the blood cells responsible for the transport of oxygen from the lungs to the tissues and carbon dioxide from the tissues to the lungs. The hemoglobin contained in the nuclei of red blood cells is the substance that operates this transport, thanks to the iron it contains, which gives these cells their color [4,5]. The iron can

be magnetized in two ways, or by contact with a magnet, or effect of an electromagnetic field. As it is known, the red blood cells contain iron atoms.

Consequently it is reasonably safe to assume that red blood cells can be electrified and magnetized, attracting one another, forming one pile and by doing so increasing the ESR. The ESR measures the fluidity of the blood, the higher the ESR, less fluid is blood. When the blood is magnetic, the ESR values rise [6].

Generally, a high ESR is interpreted as the sign of an infection. But in the case of blood the magnetic VES can be high without the presence of any infection. A result of the magnetized blood is both a lower fluidity, and a decrease in its ability to transport energy to the cells, tissues and organs.

The effects of electric and magnetic blood can be different at times with seemingly inexplicable symptoms. It's opinion of the authors that the investigation of the actions of electromagnetic fields interacting with the human body may allow the acquisition of important information on useful and sensible aspects of human response in circulatory terms.

In other words the flow of blood in the presence of a electromagnetic field gives rise to induced spiral phenomena in the blood vessel of the circulatory system. In fact, the presence of ferrous component within the blood flow determines the magnetism of the same due to external magnetic source which it's subjected. So, the magnetism causes the vertical motion phenomena that is one the most important aspects in the blood circulation.

In first approximation the sliding blood in the arteries can be described by Poiseuille's law which relates the flow rate Q of a current of a constant laminar and incompressible fluid in a rigid circular duct with constant cross section through the expression:

***Corresponding author:** Michele Buonsanti, Department DICEAM University of Reggio Calabria, Italy Via Graziella loc. Feo di Vito 89060 Reggio Calabria, Italy, E-mail: michele.buonsanti@unirc.it

Received June 12, 2013; Accepted July 09, 2013; Published July 18, 2013

Citation: Buonsanti M, Megali G, Cacciola M (2013) Electromagnetic Radiation in Bio-Tissue: A Numerical implementation. J Biomim Biomater Tissue Eng 18: 109. doi: [10.4172/1662-100X.1000109](https://doi.org/10.4172/1662-100X.1000109)

Copyright: © 2013 Buonsanti M, et al. This is an open-access article distributed under the terms of the Creative Commons Attribution License, which permits unrestricted use, distribution, and reproduction in any medium, provided the original author and source are credited.

$$Q = \frac{\pi \Delta p r^4}{8 \eta L} \quad (1)$$

Where η is the viscosity while r and L are radius and length of the cylindrical vessel, Δp is the pressure difference at the ends of the duct. Consequently, small changes in radius produce large flow variations.

In the case of vessels, with a diameter greater than 0.5 mm, the viscous behavior blood can be considered as Newtonian type; blood flows as a series of coaxial cylindrical foils, where the central layer has the maximum speed and the most external has zero speed.

The speed u will be parabolic descending from the central axis with its gradient as dv/dr and shear stress $\tau = \eta(\partial u/\partial r)$. In reality, the blood vessels are not rigid and the blood flow is not constant, but pulsatile.

From the energetic point of view, in every instant, the theorem of conservation allows the conversion of kinetic energy to pressure, depending on the change of section of the vessel. The laminar flow that is typical of the great vessels can become turbulent as it approaches the critical Reynolds number R .

In the micro-circulation blood behaves as a non-homogeneous fluid (likely structured fluid) therefore blood viscosity varies with shear rate and apparent viscosity η_{app} is influenced by the temperature of the plasma viscosity, the pH of the concentration of erythrocytes and their size and deformability [5].

For vessels whose diameter is comprised between 500 and 30 μm the value of η_{app} decreases with decreasing radius. Either way, the presence of red blood cells, in high concentration, determines the rheological behavior of the blood giving this the character of non-Newtonian fluid.

From the rheology, combined with the non-laminar flow regime, descends a physical picture for an analytical model whose actual behavior is very close to the Beltrami flow model [7]. About this last generally speaking Beltrami flow is defined by $\omega = \lambda u$, where ω is a vector field and normally represents the vorticity field, with velocity field u . The resulting problem solution is hard to obtain since great difficulties appear to Navier-Stokes closed form solution.

Following [7] a coherent approach, with our model, has been compared through helical solution for the free Maxwell equation, representing this the electromagnetic analogy of the Beltrami fields. In [7] the author find, in closed form, stable spherical formations in according to previous experiences in vorticity treating.

Problem Formulation

Electrical properties of biological materials have been a focus of interest since influences of electromagnetic waves are particularly interested by these properties [8-11].

Specifically, human tissues exposed to EM field absorb its energy and are subjected to different effects depending principally on its frequency. We focus our attention on effects produced by high frequency radiations, particularly at 2.45 GHz because of our interest in WLAN applications. The analysis can be consequentially reduced to the determination of $SAR = \sigma ||E||^2/\rho$, expressing the power absorbed per unit of mass, where σ is the conductivity of human brain tissue, ρ the density, and $||E||$ is the norm of the electric field.

Studies about the interaction of EM field with human bodies were investigated since '80s when WLAN technology did not exist yet. Advances started in '90s with more performing computers and software [1]. Studies were focused on single parts of human body (e.g., the head)

and not to the whole body since high frequency radiations. The main advantages of actual tools are the precise modeling of human head by importing MRI images and setting the parameters of different tissues. In addition, it has to model not only the direct radiation, but also the effects of scattering. FEM approach retrieves accurate results and can be exploited for multi-physics analysis, i.e., for studying the effects of EM field on the SAR and temperature of human heads.

But, in presence of large scenarios, FEM is affected by high computational complexity. In order to decrease the computational load of FEM, we reduced the in-study environment, reproducing indoor scenarios in a Ray Tracing [12,13] based environment, evaluating the EM field propagation and retaining the results for the subsequent FEM based step. Within Ray Tracing based software, we realized wireless antennas by referring to common commercial antennas. Moreover, we evaluated the EM field by placing different fictitious receivers, delimitating a volumetric area in which is supposed to stay the human head. In this way, we consider as much common situations as possible and provided a variety of results (see Table 1). Subsequently, we introduced our results in a FEM based software, where the human head has been imported by SAM Phantom provided by IEEE and IEC in their studies about SAR measurements [14-18]. Here, a cube has been modeled, containing the human head. Suitable boundary conditions have been applied to cube's surfaces, satisfying the theorem of equivalence [19] and exploiting the Ray Tracing numerical results.

In this way, we have the same EM effects on the head without modeling the whole large scenarios within the FEM software. Thus, Maxwell equations have been exploited to calculate energy filed that invests the head model. Particularly, our model solves the vector Helmholtz equation everywhere in the domain for an imposed frequency:

$$\nabla_x \mu_r^{-1} (\nabla_x E) - k_0^2 (\epsilon_r - j \frac{\sigma}{\omega \epsilon_0}) = 0 \quad (2)$$

Where μ_r is the relative permeability (1.35 [S/m]), k_0 is the free-space wave vector, and ϵ_r is the permittivity for a vacuum (56). Constant values of brain tissues have been taken from Schmid studies [20,21]. With this approach, we are able not only to evaluate EM field that invests the head model, but also the EM field inside the head. In this way we can determine also how radiation energy is absorbed by head tissues, thus calculating the SAR values for the head subdomain. The SAR value is an average over a region of either 10 [g] or 1 [g] of brain tissue, depending on national rules. This model does not calculate the average value and so it refers to the local SAR value.

The maximum local SAR value is always higher than the maximum SAR value. In our case, we calculate SAR distribution in the head both on the surface and in depth. To evaluate temperature increases, instead, Bio-heat equation has been exploited [22]:

$$\nabla \cdot (-K \nabla T) = \rho_b c_b \omega_b (T_b - T) + Q_{met} + Q_{ext} \quad (3)$$

where ρ_b is the blood density, c_b the specific heat of blood, ω_b the

Parameter	Omni-directional	Unidirectional
	Gain	5.0 [dBi]
Polarization	Vertical	Vertical
E-Plan half-power beamwidth	100.00	105.00
E-Plan first null beamwidth	170.00	165.00
H-Plane half-power beamwidth	90.00	90.00
H-Plane null beamwidth	180.00	180.00

Table 1: Parameter imposed for WLAN antenna.

perfusion rate of blood, T_b the blood temperature, Q_{met} the metabolic thermic source and Q_{ext} the spatial thermic source.

Constant values were previously set referring to Schmid's works [20,21]. Since our multi-physic approach, it has been possible to calculate directly the Q_{ext} within the FEM software package by referring to the Joule effect inside the head, exposed to EM radiation. The Bio-heat equation models the heating of the head with a heating loss due to the blood flow. This heat loss depends on the heat capacity and density of the blood, and on the blood perfusion rate. The perfusion rate varies significantly in different parts of the human body, and the Table 2 presents the values used in the present work. In order to numerically solve the approached problem, different meshes have been generated with different degrees of accuracy, depending on head sections we were interested in. But, for wave-propagation problem such ours, it is necessary to limit the mesh size according to the problem's minimum wavelength (typically five elements per wavelength to properly resolve the wave). Our main goal is to verify that the SAR values respect the international ICNIRP standards of 2 [W/kg] for head and body. Then, we want to establish the temperature increase respect to the measured SAR values.

Following figures (please refer to Figures 1-7) show the SAR and temperature variations according with different scenarios simulated and different kind of antenna propagation [22,23].

Generally, SAR distribution in head model and temperature plots draw that the areas where the increase of SAR and temperature are concentrated and where the peak values are reached.

SAR distribution, instead, allow to verify that limits are respected and study how the radiation penetrate in the model. For example, it is possible to see that the radiation penetrate mostly from the side where the antenna is positioned, but other areas are interested in temperature increasing due to the presence of reflected/scattered radiations (by roof or walls). Several simulations were carried out for analyzing the EM effects with the distance between the antenna and the head model. As we expected, in general, temperature and SAR decrease with the

Part	Perfusion rate
Brain	2×10^{-3} [(ml/s)/ml]
Bone	3×10^{-4} [(ml/s)/ml]
Skin	3×10^{-4} [(ml/s)/ml]

Table 2: Parts of human body and relatively perfusion rates.

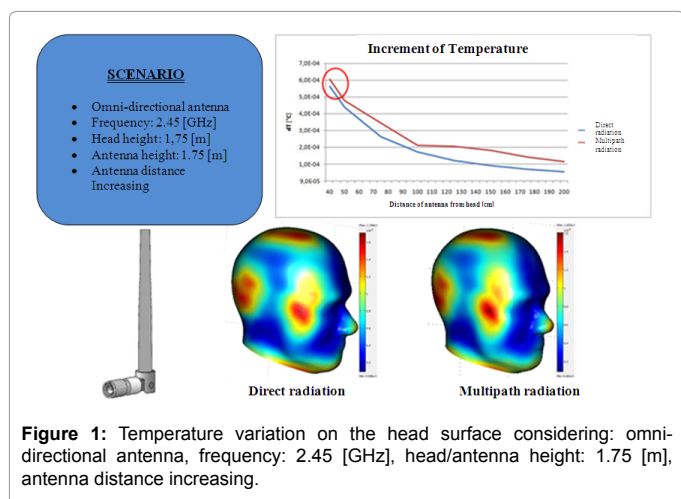


Figure 1: Temperature variation on the head surface considering: omni-directional antenna, frequency: 2.45 [GHz], head/antenna height: 1.75 [m], antenna distance increasing.

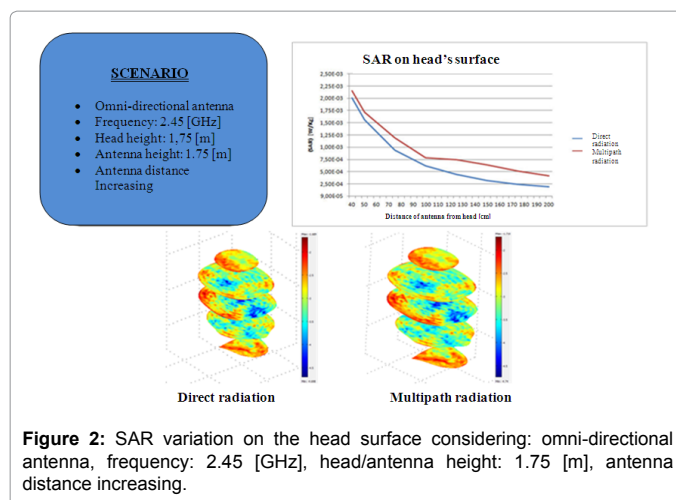


Figure 2: SAR variation on the head surface considering: omni-directional antenna, frequency: 2.45 [GHz], head/antenna height: 1.75 [m], antenna distance increasing.

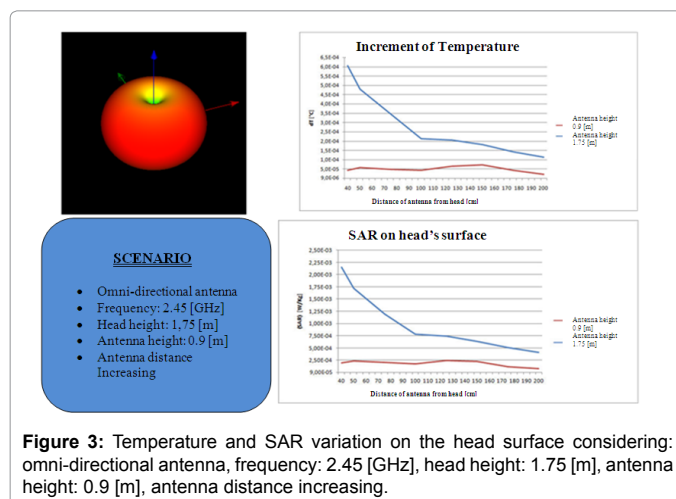


Figure 3: Temperature and SAR variation on the head surface considering: omni-directional antenna, frequency: 2.45 [GHz], head height: 1.75 [m], antenna height: 0.9 [m], antenna distance increasing.

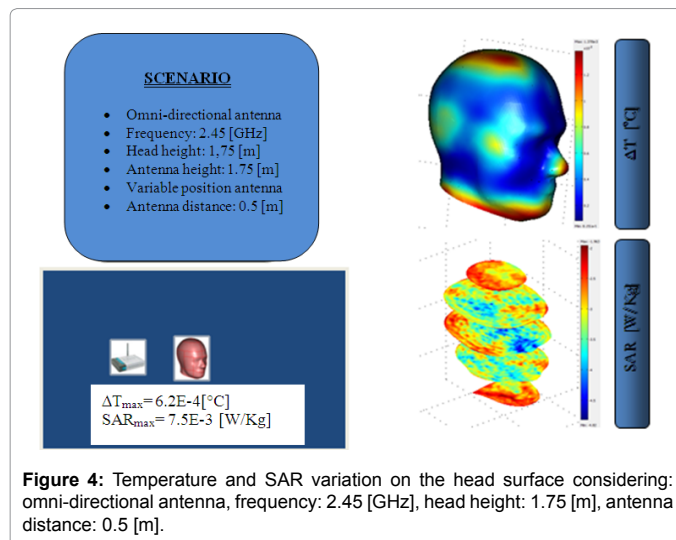
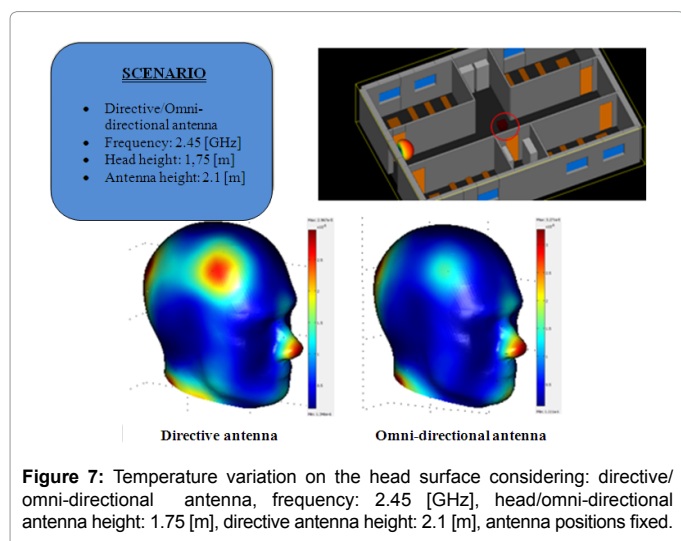
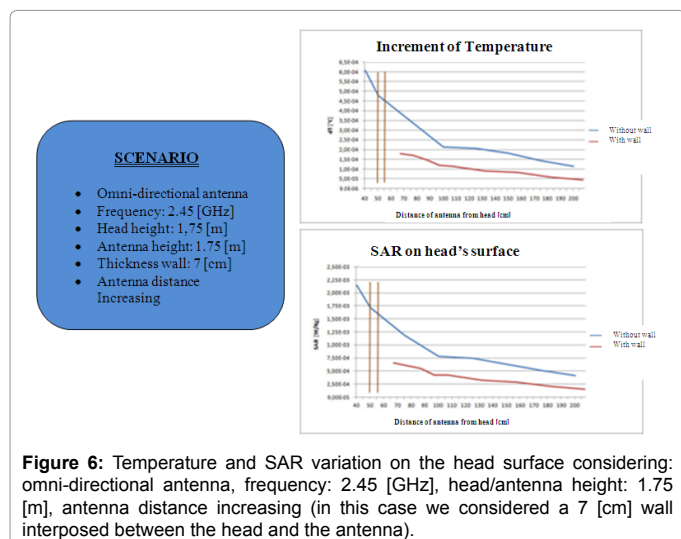
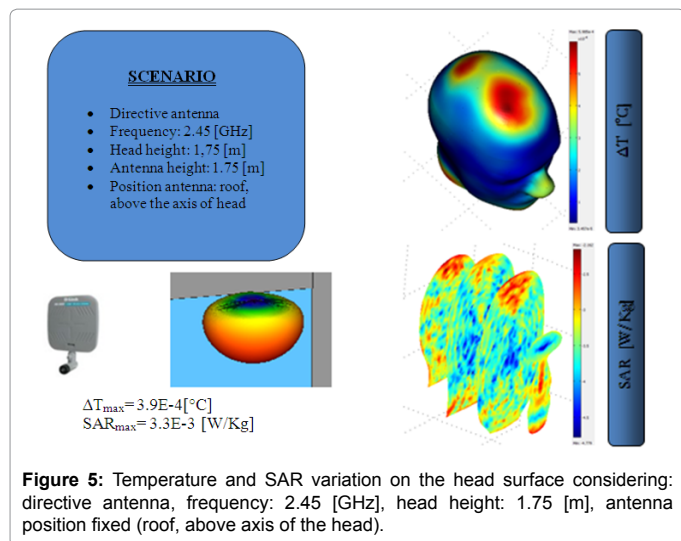


Figure 4: Temperature and SAR variation on the head surface considering: omni-directional antenna, frequency: 2.45 [GHz], head height: 1.75 [m], antenna distance: 0.5 [m].

distance, and calculated values are influenced by reflected radiation. Particularly, there is a decrement of $4\text{-}5 \times 10^{-4}$ [°C] for temperature and about $17 \times 10^{-4}\text{-}1.5 \times 10^{-3}$ [W/kg] for SAR.

We also consider the effect due to presence of 7 [cm]-thick brick



wall, positioned between the antenna and the head model, in order to simulate the case of two rooms close each other. The presence of the

wall causes a decrement of values of $4.5 \cdot 10^{-4} [^{\circ}C]$ for temperature and $1.5 \cdot 10^{-3} [W/kg]$ for SAR, according to the fact that quite part of radiation is absorbed by the wall. Many other cases with antenna positioned in different placed were examined, but never registering values higher than the standard limit. For instance, we examined the case of antenna positioning on a desk close to a user: in this case, simulations showed a temperature increment at the bottom part of the head near the chin, but values do not exceed standard limits.

All these cases are referred to an omni-directional antenna. Considering directive antennas, peaks values of temperature and SAR are positioned in correspondence of axis of maximal directivity. We considered also these cases, showing that calculated values were a little bit higher than the case of omni-directional antenna, and temperature increments are more concentrated in the areas of direct exposure. On the contrary, when user is not positioned in correspondence of the maximum directivity axis, omni-directional antennas have registered values higher than directive ones. For instance, in this last case, at a distance of 2.0 [m], the increment of temperature is $4 \cdot 10^{-6} [^{\circ}C]$ with a directive antenna and $10^{-5} [^{\circ}C]$ with an omni-directional antenna.

Conclusions

In this study, we analyzed the effects of EM field exposure to human head from WLAN instrumentations like Access-Point or Hot-Spot. Our interest was focused on SAR evaluation and temperature increase due to EM-wave propagation. Based on numerical simulations carried out with a joint Ray-Tracing and FEM based approach, interaction between EM field and head model has been investigated. For this reason, different scenarios have been implemented. The proposed method provides a good overall accuracy in determining these effects, as our simulations demonstrate. Numerical models remarked that the distance between antenna and user is the most important parameter for determining the intensity of SAR and temperature increments as well as the exposed area of the human head. Within this framework, we have analyzed field penetration: the radiation penetrates till 1 [cm] of deepness, especially when the antenna is positioned in front of the user (in this case, the eyes, for their composition, are the organs that absorb most part of radiation).

Anyway, results of our simulations never overcame the thresholds imposed by international laws.

The proposed study shows preliminary results, since we consider general cases. Further improvements could analyze particular situations and investigate other wireless technologies using different frequency ranges, in order to establish the impact on human safety.

References

1. Bernardi P, Cavagnaro M, Pisa S (1997) Assessment of the potential risk for humans exposed to millimeter-wave wireless lans: the power absorbed in the eye. *Wireless Networks* 3: 511-517.
2. Kuhn S, Urs L, Kramer A, Kuster N (2007) Assessment Methods for Demonstrating Compliance With Safety Limits of Wireless Devices Used in Home and Office Environments. *IEEE Trans on Electromagnetic Compatibility* 49: 519-525.
3. Bernardi P, Cavagnaro M, Pisa S, Piuze E (1998) SAR distribution and temperature increase in an anatomical model of the human eye exposed to the field radiated by the user antenna in a wireless LAN. *IEEE Trans on Microwave Theory and Techniques* 46: 2074-2082.
4. Fung YC (1990) *Biomechanics: Circulation*, Springer, New York, 3.
5. Fung YC (1990) *Biomechanics: Motion, flow, stress and growth*, Springer, New York, 2.

6. Foster KR, Schwan HP (1995) Dielectric properties of tissues. In: Polk C, Postow E (Eds.), Handbook of Biological Effects of Electromagnetic Fields (2nd edn), CRC Press, 1996.
7. Kwang-Hua Chu R (2004) Possible Ball like formations of the Beltrami Flow Field, *Meccanica*, 39: 181-186.
8. Levallois P (1999) Study review of hypersensitivity of human subjects to environmental electric and magnetic field exposure. Report to public Health Institute, California Depart. Health Service.
9. Salford LG, Brun AE, Eberhardt JL, Malmgren L, Persson BR (2003) Nerve cell damage in mammalian brain after exposure to microwaves from GSM mobile phones. *Environ Health Perspect* 111: 881-883.
10. Preece AW, Iwi G, Davies-Smith A, Wesnes K, Butler S, et al. (1999) Effect of a 915-MHz simulated mobile phone signal on cognitive function in man. *Int J Radiat Biol* 75: 447-456.
11. Henshaw DL, Ross AN, Fews AP, Preece AW (1996) Enhanced deposition of radon daughter nuclei in the vicinity of power frequency electromagnetic field, *International Journal Radiation Biology* 69: 25-38.
12. Glassner A (1989) In: *Academi Press*, New York, NY, USA.
13. Shirley P, Morley KR (2001) In: *Peters AK* (2nd edn), New Jersey, USA (2001)
14. (1980) International Commission on Radiation Units and Measurements, \ "Radiation quantities and units," ICRU Report 33 (Bethesda, MD: ICRU).
15. (2003) Electronics Communications Committee (ECC) within the European Conference Postal and Telecommunications Administrations. "Measuring Non-ionizing Electromagnetic Radiation (9 kHz-300 GHz)".
16. (2005) Human Exposure to Radio Frequency Fields From Handheld and Body-Mounted Wireless Communication Devices-Human Models, Instrumentation and Procedures, Part 1: Procedure to Determine the Specific Absorption Rate (SAR) for Handheld Devices Used in Close Proximity to the Ear (Frequency Range of 300MHz to 3 GHz), IEC 62209 Part 1.
17. (2003) IEEE Recommended Practice for Determining the Peak Spatial-Average Specific Absorption Rate (SAR) in the Human Head From Wireless Communications Devices: Measurement Techniques, IEEE Standard 1528-2003.
18. (2001) Basic Standard for the Measurement of Specific Absorption Rate Related to Human Exposure to Electromagnetic Fields From Mobile Phones (300 MHz to 3 GHz), CENELEC EN 50361.
19. Franceschetti G (1983) Boringhieri, Turin, Italy (in Italian language).
20. Schmid G, Neubauer G, Mazal PR (2003) Dielectric properties of human brain tissue measured less than 10 h postmortem at frequencies from 800 to 2450 MHz. *Bioelectromagnetics* 24: 423-430.
21. Schmid G, Neubauer G, Illievich UM, Alesch F (2003) Dielectric properties of porcine brain tissue in the transition from life to death at frequencies from 800 to 1900 MHz. *Bioelectromagnetics* 24: 413-422.
22. Megali G (2011) PhD Thesis.
23. Megali G, Cacciola M (2012) *Mondo Digitale* Vol. 44.

Citation: Buonsanti M, Megali G, Cacciola M (2013) Electromagnetic Radiation in Bio-Tissue: A Numerical implementation. J Biomim Biomater Tissue Eng 18: 109. doi: [10.4172/1662-100X.1000109](https://doi.org/10.4172/1662-100X.1000109)

Submit your next manuscript and get advantages of OMICS Group submissions

Unique features:

- User friendly/feasible website-translation of your paper to 50 world's leading languages
- Audio Version of published paper
- Digital articles to share and explore

Special features:

- 250 Open Access Journals
- 20,000 editorial team
- 21 days rapid review process
- Quality and quick editorial, review and publication processing
- Indexing at PubMed (partial), Scopus, EBSCO, Index Copernicus and Google Scholar etc
- Sharing Option: Social Networking Enabled
- Authors, Reviewers and Editors rewarded with online Scientific Credits
- Better discount for your subsequent articles

Submit your manuscript at: <http://www.omicsonline.org/submission>